A finite volume scheme for the transport of radionucleides in porous media

Eric Chénier, Robert Eymard, Xavier Nicolas

A finite volume scheme for the transport of radionucleides in porous media

E. Chénier, R. Eymard and X. Nicolas
Université de Marne-la-Vallée *

Abstract. This paper presents the use of a finite volume scheme for the simulation of the COUPLEX1 Test case. We first show that the results of the simulation can be mainly predicted thanks to an analysis of the data. We then give the formulation of a finite volume scheme, yielding accurate and stable results for a low computational cost. We finally present some of the numerical results, comparing the explicit MUSCL scheme and the implicit scheme with variable upwinding according to the local diffusion.

Keywords: COUPLEX1, finite volume scheme, variable Péclet number

AMS Subject Classifications:: 35K65, 35K55

1. Introduction

The COUPLEX-1 Test case (ANDRA, 2001) is a benchmark of numerical techniques designed for the simulation of the transport of contaminants by the water flowing through a porous medium. Since the goal is more to compare numerical methods than to improve the engineering study, the geological configuration is simplified in a four-layer cross-section. Nevertheless, within the framework of an engineering study, the numerical results are necessarily compared to simple calculations without a computer, even under coarse approximations. Thus we first present in Section 2 an approximate analysis which gives some indications on the qualitative results which can be a priori expected from the data of the problem. We secondly give, in Section 3, a short discussion on the appropriate numerical schemes. We then present in Section 4 some of the numerical results which have been obtained using, on the one hand, an explicit MUSCL scheme for the transport part of the problem, on the other hand, an implicit scheme with variable upwinding according to the local diffusion.

* Laboratoire d'Etude des Transferts d'Energie et de Matière, UMLV (`http://www-letem.univ-mlv.fr`) 5, boulevard Descartes - Champs-sur-Marne - 77454 Marne-la-Vallée Cedex 2, FRANCE

2. Approximate analytical study

We first begin with a global study of the problem, mainly using hand calculations. Such a procedure is commonly followed in industrial contexts. The data are recalled, for the sake of completeness, in the appendix of this paper.

2.1. Characteristics of the velocity field

Since the geological description of the domain reduces to two highly permeable thick layers (limestone and dogger) separated by two weakly permeable thin layers (marl and clay), (see figure 1) the hydraulic head field can be approximately evaluated using the volumic flow conservation in a 1D medium for each of the permeable layers:

• this yields a constant head gradient in the dogger layer, leading to a linearly decreasing head from the bottom right vertical boundary to the bottom left vertical boundary,

• this also yields the following equation for the hydraulic head in the limestone layer (since the lower boundary of this layer is tilted, the area of the vertical sections is given by a linear function of the horizontal position x)

$$\left(300 - \frac{300 - 245}{25000}\ x\right) \frac{\partial H}{\partial x} = \text{constant}, \tag{1}$$

with $x = 0$ at the left boundary and $x = 25000\ m$ at the right boundary. Therefore a logarithmic head profile is available in the limestone layer, decreasing from the right to the left.

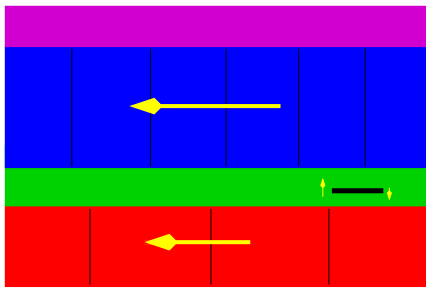

Figure 1. A priori contour levels of the piezometric head

It yields the following values for the hydraulic head in the dogger layer:

$$H(x) = 286 + \frac{289 - 286}{25000}\ x, \tag{2}$$

also available at the bottom horizontal boundary of the clay layer, and

$$H(x) = 200 + \frac{110}{\ln(245/300)} \ln\left(1 - \frac{300 - 245}{300 \times 25000}\, x\right). \qquad (3)$$

in the limestone layer, also available at the top tilted boundary of the clay layer.

Therefore, using equations (2) and (3), the piezometric head H is expected to be approximately equal to $H_{b-l} = 288.2\ m$ at the bottom boundary of the clay layer and $H_{t-l} = 278.9\ m$ at the top boundary of the clay layer at the level of the left side of the repository ($x = 18440\ m$). In the same way, the piezometric head approximately equals $H_{b-r} = 288.6\ m$ at the bottom boundary and $H_{t-r} = 294.0\ m$ at the top boundary of the clay layer at the level of the right side of the repository ($x = 21680\ m$).

Since the vertical dimension of the domain is much smaller than the horizontal one, the vertical flow will predominate in the clay layer, and the Darcy velocity can therefore be computed using the difference of pressure between the top boundary and the bottom boundary on a vertical line. Thus, the change of sign of this difference along the repository confirms that its location has been chosen such that the velocity field vanishes at the level of the repository.

Taking this result into account and since the thickness of the clay layer varies between 135.6 m and 142.7 m at the level of the repository, the maximum upward velocity at the left side of the repository is about $u_{max-l} = -3.15 \times 10^{-6}\ \frac{278.9-288.2}{135.6} \simeq 2.2 \times 10^{-7}\ m/year$ and the maximum downward velocity at its right side is about $u_{max-r} = -3.15 \times 10^{-6}\ \frac{294.0-288.6}{142.7} \simeq -1.2 \times 10^{-7}\ m/year$.

The x-coordinate at which the vertical pressure gradient in the clay is vanishing is then given by $x = 18440 + (21680 - 18440) * \frac{2.2}{2.2+1.2} \simeq 20500\ m$. The accuracy of this value should be discussed, since a small uncertainty on the piezometric head leads to a more important uncertainty on this position.

2.2. Characteristic times for the iodine transport

From the previous values of piezometric heads (H_{b-l} and H_{t-l}) and velocities (u_{max-l} and u_{max-r}), one can guess different characteristic time values:

- let $d_t = 85.6\ m$ be the shorter distance between the repository and the top boundary of the clay layer; the convective time of iodine

to this boundary is $\Delta t_{conv-t-i} = \frac{\omega_i R_i d_t}{|u_{max-l}|}$, which is about $\frac{10^{-3}\times 1\times 85.6}{2.2\times 10^{-7}} = 3.9\times 10^5$ *years*;

• let $d_b = 44$ *m* be the distance between the repository and the bottom boundary of the clay layer; the convective time of iodine to this boundary is $\Delta t_{conv-b-i} = \frac{\omega_i R_i d_b}{|u_{max-r}|}$, which is about $\frac{10^{-3}\times 1\times 44}{1.2\times 10^{-7}} = 3.6\times 10^5$ *years*;

• the diffusion time in the clay layer calculated from the repository to the top boundary is about $\Delta t_{diff-t-i} = \frac{\omega_i R_i d_t^2}{D_i} = \frac{10^{-3}\times 1\times 85.6^2}{9.5\times 10^{-7}} = 7.7\times 10^6$ *years*;

• the diffusion time in the clay layer calculated from the repository to the bottom boundary is about $\Delta t_{diff-b-i} = \frac{\omega_i R_i d_b^2}{D_i} = \frac{10^{-3}\times 1\times 44^2}{9.5\times 10^{-7}} = 2.0\times 10^6$ *years*;

• the convective time in the dogger layer from the repository to the left bottom boundary of the computational domain (distance $d_l = 18440$ *m*) is about $\Delta t_{conv-dog-i} = \frac{\omega_i R_i d_l}{K_{dog}\nabla H} = \frac{0.1\times 1\times 18440}{25.2\times(288.2-286)/18440} = 6.1\times 10^5$ *years*;

• the convective time in the limestone layer from the repository to the left middle boundary of the computational domain (distance $d_l = 18440$ *m*) is about $\Delta t_{conv-lim-i} = \frac{\omega_i R_i d_l}{K_{lim}\nabla H} = \frac{0.1\times 1\times 18440}{6.3\times(278.9-200)/18440} = 6.8\times 10^4$ *years*.

This first estimation of the characteristic times of the iodine transport in the clay layer shows that $\Delta t_{diff-t-i} > \Delta t_{diff-b-i} > \Delta t_{conv-t-i} > \Delta t_{conv-b-i}$. Therefore, in this layer, the diffusive transport is slower than the convective transport and iodine reaches the bottom boundary of the clay layer before the top boundary. Furthermore, since the characteristic times in the clay layer and the convective times in the limestone and dogger layers are much smaller than the half life of iodine (1.57×10^7 *years*), nearly the full amount of the iodine which will reach the limestone and dogger layers will propagate until the left boundary of the computational domain, before the decay of the iodine radioactivity begins.

2.3. Characteristic times for the plutonium transport

The characteristic time values for plutonium are quite different:

• the convective time of plutonium to the top boundary of the clay layer is about $\Delta t_{conv-t-p} = \frac{\omega_p R_p d_t}{u_{max-l}} = \frac{0.2\times 10^5\times 85.6}{2.2\times 10^{-7}} = 7.8\times 10^{12}$ *years*;

• the convective time of plutonium to the bottom boundary of the clay layer is about $\Delta t_{conv-b-p} = \frac{\omega_p R_p d_b}{u_{max-r}} = \frac{0.2\times 10^5\times 44}{1.2\times 10^{-7}} = 7.3\times 10^{12}$ *years*;

• the diffusion time of plutonium in the clay layer calculated from the repository to the top boundary is about $\Delta t_{diff-t-p} = \frac{\omega_p R_p d_t^2}{D_p} = \frac{0.2\times10^5\times85.6^2}{4.4\times10^{-4}} = 3.3\times10^{11}\ years$;

• the diffusion time of plutonium in the clay layer calculated from the repository to the bottom boundary is about $\Delta t_{diff-b-p} = \frac{\omega_p R_p d_b^2}{D_p} = \frac{0.2\times10^5\times44^2}{4.4\times10^{-4}} = 8.8\times10^{10}\ years$;

Therefore, the convective times, diffusive times and half life time ($3.76\times10^5\ years$) of plutonium are very different. The main mechanism is therefore the decay of plutonium before it is convected or diffused. No significative amount of radioactive plutonium can reach the boundaries of the clay layer.

2.4. Conclusion of this first survey

We have been able to give coarse predictions of the amount of radionucleides which reaches the left boundary of the domain, using only very simple calculations. This is mainly due to the fact that the data are here very simple, compared to realistic ones. However, from our point of view, such a procedure must always take place before any numerical study, because it gives the physical key points which help to validate the numerical results.

3. Numerical schemes

The following analysis of the required numerical schemes can be made.

• The problem is a convection-diffusion problem with a heterogeneous anisotropic diffusion matrix (due to the expression of the dispersion matrix). Therefore some advantages can be drawn from a $P1$-finite element formulation (linear fields on triangles), viewed as a finite volume method on the dual mesh (given by orthogonal bissectors) for the convection terms (Eymard, Gallouët, Herbin, 2000).

• The high ratio between the horizontal and the vertical dimensions implies to use meshes designed for this purpose.

• The dispersion terms are in competition with the numerical diffusion provided by the first order upstream weighted finite volume scheme for the convection term (a centered scheme cannot be used everywhere because of the constrast between the different rock properties within the domain). The low vertical size of the dispersion matrix implies that this term can be accurately handled in the vertical direction, but that it is necessarily partly increased in the horizontal direction.

We have therefore used the following schemes. A $P1$-finite element scheme is used to solve the equation

$$-\text{div } \Lambda \nabla H = 0, \tag{4}$$

in which we denote by Λ isotropic heterogeneous value of the permeability. We write this scheme as follows

$$-\sum_{L \in N_K} T_{KL}(H_L - H_K) = 0, \tag{5}$$

where K is a vertex of the mesh, and N_K is the set of the vertices of all triangles having K as a vertex (see figure 2, left).

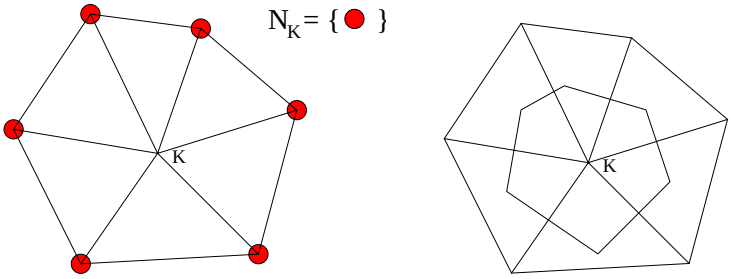

Figure 2. Triangular mesh: neighbours of a vertex (left), dual mesh (right).

In equation (5), we denote by T_{KL} the term of the rigidity matrix, given by

$$T_{KL} = -\int_\Omega \nabla \varphi_K(x) \cdot \Lambda(x) \nabla \varphi_L(x) dx, \tag{6}$$

denoting by φ_K the $P1$ basis function, which is linear in each triangle, continuous, whose value is 1 at the vertex K and 0 at all the other vertices. As we remarked above, ∇u (and therefore of $D(\nabla u)$) is constant in each triangle. Note that the $P1$ finite element scheme can also be seen as a finite volume scheme on the dual mesh: see figure 2 (right), which shows the Voronoï mesh related to the triangular mesh of figure 2 (left).

We can now write, in the same way, a finite volume scheme for the concentrations, setting the volumic flow between two control volumes around vertices K and L by

$$Q_{K,L} = T_{KL}(H_K - H_L) \tag{7}$$

and setting initial values for concentrations

$$c_K^{(0)} = 0. \tag{8}$$

The scheme writes, at a given time step n,

$$\begin{array}{l} \omega_K m_K \left[(c_K^{(n+1)} - c_K^{(n)})/\Delta t + \lambda c_K^{(n+1)} \right] \; + \\ \displaystyle\sum_{L \in N_K} \left[\begin{array}{l} c_{K,L}^{(m)} Q_{K,L}^{+} - c_{L,K}^{(m)} Q_{L,K}^{+} \\ -D_{KL}(c_L^{(m)} - c_K^{(m)}) \end{array} \right] \qquad = f_K^{(n)} \end{array} \tag{9}$$

where the diffusive coefficient D_{KL} is given using the dispersion matrix by

$$D_{KL} = -\int_\Omega \nabla\varphi_K(x) D(\nabla H)(x) \nabla\varphi_L(x) dx. \tag{10}$$

In (9), m_K is the area of the control volume K around the vertex K (it is in fact taken as 1/3 of the areas of all the neighbouring triangles), ω_K gathers the effects of the effective porosity and of the retardation factor, $f_K^{(n)}$ denotes the source term, and in (10), $D(\nabla H)(x)$ denotes the dispersion matrix in the domain as a function of the approximate gradient of hydraulic head. An explicite scheme is obtained with $m = n$ (the time step Δt is then bounded to respect a CFL value: this bound is approximately 77 years for the mesh which is used below) and an implicite one is given by $m = n + 1$ (in this case, the time step Δt is ajusted along the simulation to yield maximum variations of concentration equal to 10^{-4}). We now have to define the way of computing the values of the interface concentration $c_{K,L}^{(m)}$ used in (9).

• In the explicite case we use a MUSCL scheme. We first compute an approximate value for $\nabla c^{(n)}$ in all the control volumes around the vertices. We then limit this gradient in order to obtain that all the values

$$c_{K,L}^{(m)} = c_K^{(n)} + \frac{1}{2} \tilde{\nabla} c_K^{(n)} \cdot \vec{KL} \tag{11}$$

be between $c_K^{(n)}$ and $c_L^{(n)}$, for any pair of vertices of the same triangle (in (11), we denote by $\tilde{\nabla} c_K^{(n)}$ the limited gradient).

• In the implicite case, the following upwinding scheme can be used:

$$c_{K,L}^{(m)} = c_K^{(n+1)}. \tag{12}$$

Scheme (12) will be referred, in the following, as the "upwinding" implicit scheme. Taking into account some discussions during the Couplex Workshop, we introduced the scheme

$$c_{K,L}^{(m)} = (1 - \alpha_{K,L}) c_K^{(n+1)} + \alpha_{K,L} c_L^{(n+1)}, \tag{13}$$

for all pairs K, L of neighbouring vertices. In (13), $\alpha_{K,L}$ is given by

$$Q^+_{K,L}\alpha_{K,L} = \min\left(D_{KL}, \frac{1}{2}Q^+_{K,L}\right) \tag{14}$$

Scheme (13)-(14) thus only adds the minimum needed numerical diffusion for the stability of the scheme (which thus satisfies a condition on the local Péclet number). Note that (13)-(14) can even add some diffusion if $D_{KL} < 0$ (which can occur with a non diagonal dispersion matrix), yielding a strong respect of the local maximum principle. This scheme will be referred, in the following, as the "centered" implicit scheme.

Using a direct Gauss band solver for all linear systems, we have obtained the following run times on a PC computer (clock frequency 500 MHz):

• using the implicit scheme, the run-times have been of about 1 hour and 10 minutes for 23906 vertices,

• a 5 hours computing time has been necessary for the MUSCL explicit scheme on the same grid.

4. Numerical results

We present hereafter the main results concerning the piezometric head field and the Iodine transport (in agreement with section 2, the Plutonium transport is not numerically significant).

4.1. Numerical results: the piezometric head field

Figure 3 shows the grid used, and contour levels for the piezometric head (a value equal to 180 m is given at the upper left corner, then the contour levels 196, 212, 228, 244, 260, from 276 to 292 with step 1, 308, 324 m are shown from the left to the right, and a value equal to 340 m is given at the upper right corner).

The obtained values of H are very closed to that which have been given in Section 2 in the limestone and dogger layers (the difference with equations (2) and (3) being lower that 1.5 m).

4.2. Numerical results for Iodine transport

There is no contour levels at time = 200 *years*. The contour levels $c = 10^{-12}, 10^{-10}, 10^{-8}, 10^{-6}, 10^{-4}$ for the times 10110, 50110, 10^6, 10^7 *years* within the three schemes (explicite, upwinding implicite, centered implicite) are given in Figures 4 to 7 (decreasing from the repository to the boundary of the domain). The explicit MUSCL scheme and the

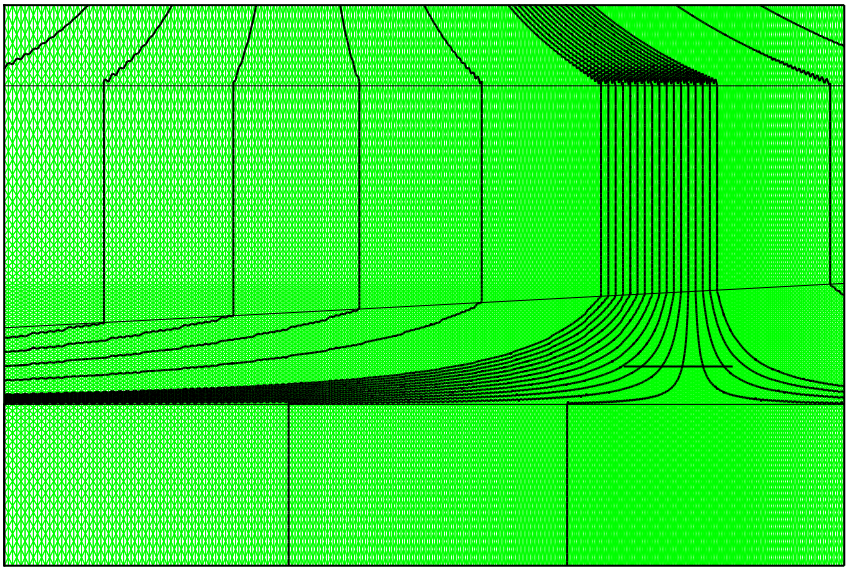

Figure 3. Contour levels of the piezometric head.

centered implicit scheme seem to be less diffusive than the upwinding implicit scheme.

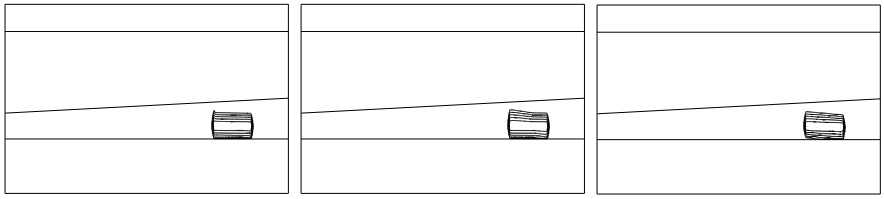

Figure 4. Contour levels of iodine concentration at time 10110 *years* (explicit MUSCL (left), upwinding implicit (middle) and centered implicit (right))

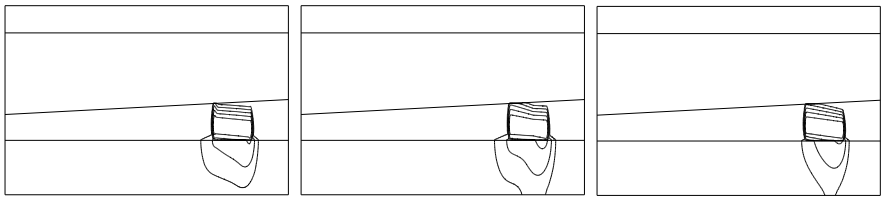

Figure 5. Contour levels of iodine concentration at time 50110 *years* (explicit MUSCL (left), upwinding implicit (middle) and centered implicit (right))

In Figure 8, we have shown separately the four cumulative Iodine amounts obtained by integration of the fluxes with respect to time (from the clay layer to the limestone and dogger layers, accross the top

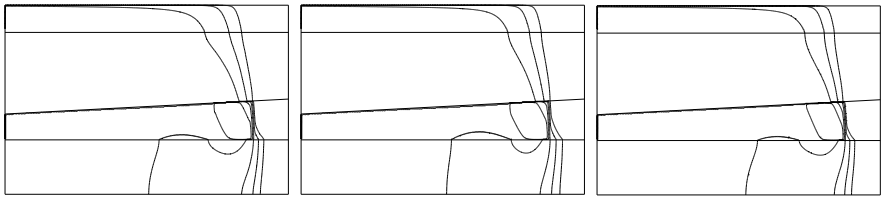

Figure 6. Contour levels of iodine concentration at time 10^6 *years* (explicit MUSCL (left), upwinding implicit (middle) and centered implicit (right))

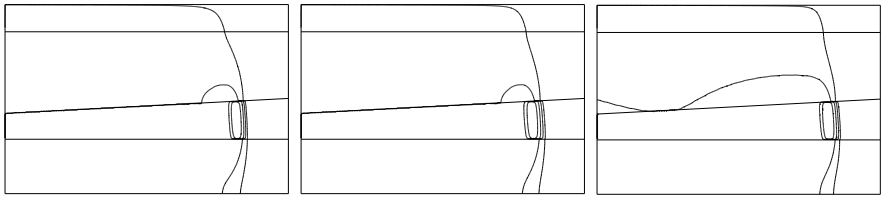

Figure 7. Contour levels of iodine concentration at time 10^7 *years* (explicit MUSCL (left), implicit upwinding upwinding implicit (middle) and centered implicit (right))

and bottom left boundaries), in order to check the qualitative results based on the characteristic times. The obtained results thus appear to be in full agreement with the first survey of the problem.

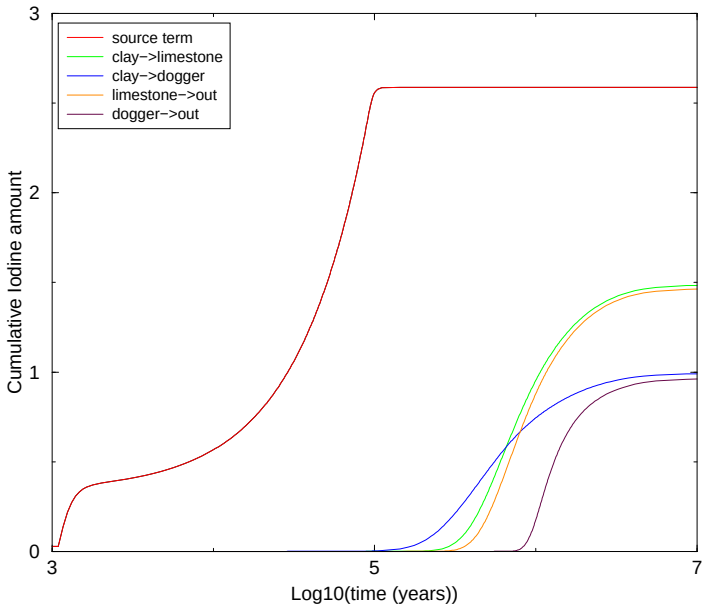

Figure 8. Cumulative Iodine amount

5. Concluding remarks

On the COUPLEX-1 Test case, a first hand computation survey of the problem can give the essential results: nearly all the iodine reaches the left boundary, and nearly no amount of plutonium can reach the boundaries of the clay layer. This shows that if the main point of engineering studies is the uncertainties evaluations, simple analytical models must also be used for the evaluation of the mass transfers.

A more accurate is nevertheless usefull. For this purpose, the finite volume scheme that we have used here appear to be efficient, stable and cheap. However, COUPLEX-1 problem has been carefully designed in order that the mathematical aspects were well posed. This can be different with more realistic data.

References

ANDRA: http://www.andra.fr/couplex/.

Eymard, R., Gallouët, T., Herbin, R.: 'Finite Volume Methods', *Handbook of Numerical Analysis, P.G. Ciarlet and J.L. Lions. eds.*, **VII** pp 723–1020, 2000.

Appendix: Data of the Couplex1 Test cas

COUPLEX1 Test Case
Nuclear Waste Disposal Far Field Simulation

January 25, 2001

Abstract

This first COUPLEX test case is to compute a simplified Far Field model used in nuclear waste management simulation. From the mathematical point of view the problem is of convection diffusion type but the parameters are highly varying from one layer to another. Another particularity is the very concentrated nature of the source, both in space and in time.

1 Introduction

The repository lies at a depth of 450m (meters) inside a clay layer which has above it a layer of limestone and a layer of marl and below it is a layer of dogger limestone. Water flows slowly (creeping flow) through these porous media and convects the radioactive materials once the containers leak; there is also a dilution effect which in mathematical terms is similar to diffusion. The problem has two main difficulties:

1. The radioactive elements leak from the containers, into the clay, over a period that is small compared with the millions of years over which convection and diffusion are active.
2. The convection and diffusion constants are very different from one layer to another; for instance, in the clay layer there is almost no convection while, in the other layers, diffusion and convection are both important.

2 The Geometry

In this first test case, the computation is restricted to a 2D section of the disposal site. Thus, the computational domain is in a rectangle $\mathcal{O} =]0,25000[\times]0,695[$ in meters. The layers of dogger, clay, limestone, and marl are located as follows (with the origin taken at the bottom left corner of the rectangle):

- dogger $0 < z < 200$
- clay lies between the horizontal line $z = 200$ and the line from $]0,295[$ to $]25000,350[$
- limestone lies between the line from $]0,295[$ to $]25000,350[$ and the horizontal line $z = 595$
- marl $595 < z < 695$.

The repository, denoted by R, is modeled by a uniform rectangular source in the clay layer:

$$R = \{(x,z) \in]18440,21680[\times]244,250[\}$$

The geometry is summarized on figure 1 below. For this domain the computation should be carried for $t \in]0,T[$ with $T = 10^7$ years.

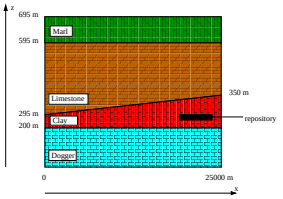

Figure 1: *Geometry of computational domain*

3 The Flow

It is assumed that all rock layers are saturated with water and that boundary loads are stationary so that the flow is independent of time. Darcy's law gives the velocity $\mathbf{u}$ in terms of the hydrodynamic load $H = P/\rho g + z$:

$$\mathbf{u} = -K\nabla H \tag{1}$$

where the permeability tensor K, assumed constant in each layer is given in Table 1, P is the pressure and g is Newton's constant. Conservation of mass ($\nabla \cdot (\rho \mathbf{u}) = 0$, with the density ρ assumed constant) implies that

$$\nabla \cdot (K\nabla H) = 0 \quad \text{in } \mathcal{O} \tag{2}$$

	Marl	Limestone	Clay	Dogger
K (m/year)	3.153e-5	6.3072	3.1536e-6	25.2288

Table 1: *Permeability tensor in the four rock layers*

On the boundary, conditions are:

$$\begin{aligned}
&H = 289 && \text{on }]25000[\times]0,200[\,,\\
&H = 310 && \text{on }]25000[\times]350,595[\,,\\
&H = 180 + 160z/25000 && \text{on }]0,25000[\times]695[\,,\\
&H = 200 && \text{on } \{0\} \times]295,595[\,,\\
&H = 286 && \text{on } \{0\} \times]0,200[\,,\\
&\frac{\partial H}{\partial n} = 0 && \text{elsewhere.}
\end{aligned}$$

4 The Radioactive Elements

We are considering two species of particular interest, Iodine 129 and Plutonium 242. Both escape from the repository cave into the water and their concentrations C_i, $i = 1,2$ is given by two independent convection-diffusion equations:

$$R_i\omega_i \frac{\partial C_i}{\partial t} + \lambda_i C_i - \nabla \cdot (\mathbf{D}_i \nabla C_i) + \mathbf{u} \cdot \nabla C_i = f_i \quad \text{in } \mathcal{O} \times]0,T[\quad i = 1,2. \tag{3}$$

where

- R_i is the latency Retardation factor, with value 1 for ^{129}I, 10^5 for ^{242}Pu in the clay and 1 elsewhere for both Iodine and Plutonium;
- the effective porosity ω_i is equal to 0.001 for ^{129}I, 0.2 for ^{242}Pu in the clay layer and 0.1 elsewhere for both;
- $\lambda_i = \log 2/T_i$ with T_i being the half life time of the element : $1.57\ 10^7$ for ^{129}I, $3.76\ 10^5$ for ^{242}Pu (in years);
- The effective diffusion/dispersion tensors $\mathbf{D}_i$ for any species $i = 1,2$ depend on the Darcy velocity as follows:

$$\mathbf{D}_i = d_{m,i} I + |\mathbf{u}| \left[\alpha_{l,i} E(\mathbf{u}) + \alpha_{t,i} (I - E(\mathbf{u})) \right]$$

with

$$E_{kl}(\mathbf{u}) = \frac{u_k u_l}{|\mathbf{u}|^2},$$

and with the coefficients, assumed constant in each layer, given in Table 2 below.

	^{129}I			^{242}Pu		
	$d_{m,i}$ (m^2/year)	$\alpha_{l,i}$(m)	$\alpha_{t,i}$(m)	$d_{m,i}$(m^2/year)	$\alpha_{l,i}$(m)	$\alpha_{t,i}$(m)
Dogger	5.0e-4	50	1	5.0e-4	50	1
Clay	9.48e-7	0	0	4.42e-4	0	0
Limestone	5.0e-4	50	1	5.0e-4	50	1
Marl	5.0e-4	0	0	5.0e-4	0	0

Table 2: *Diffusion/dispersion coefficients for the radioactive elements in the 4 layers*

In this test case, the values of the source terms f_i, $i = 1,2$ in the repository R are given in tabulated form in separately provided data files. The source terms are assumed to be spatially uniformly spread out in all the repository R. It is assumed that there is no source outside the repository (f_i, $i = 1,2$ in $\mathcal{O} \setminus \bar{R}$). The dependence in time is shown on figure 2, for illustrative purposes. The structure of the data file is described in appendix A.

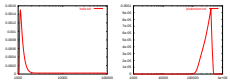

Figure 2: *Release of Iodine and Plutonium as a function of time*

4.1 Initial and Boundary Conditions

We call time zero the time when the containers begin to leak and the radioactive elements to spread, hence the initial values of the concentration C_i are zero at time zero.

Boundary conditions for the transport of any nuclide $i = 1,2$ are

$$\begin{aligned}
&\frac{\partial C_i}{\partial x} = 0 && \text{on } \{0\} \times]295,595[\\
&\frac{\partial C_i}{\partial x} = 0 && \text{on } \{0\} \times]0,200[\\
&\mathbf{D}_i \nabla C_i \cdot \mathbf{n} - C_i \mathbf{u} \cdot \mathbf{n} = 0 && \text{on }]0,25000[\times \{0\}\\
&C_i = 0 && \text{elsewhere on the boundary.}
\end{aligned}$$

where $\mathbf{n}$ is the outward normal to the vertical line $\{0\} \times]0,695[$

5 Output requirements

The following output quantities are expected from the simulations(both tables and graphical representations):

- Contour levels of C_i at times 200, 10110, 50110, 10^4, 10^7 years (the following level values should be used: 10^{-7}, 10^{-6}, 10^{-5}, 10^{-4}, 10^{-3});
- Pressure field (10 values uniformly distributed between 180 and 310);
- Darcy velocity field, along the 3 vertical lines given by $x = 50$, $x = 12500$, $x = 20000$, using 100 points along each line;
- Places where the Darcy velocity is zero;
- Cumulative total flux through the top and the bottom clay layer boundaries, as a function of time;
- Cumulative total fluxes through the left boundaries of the dogger and limestone layers;
- The discretization grid of the domains and the time stepping used in the simulations should also be given.

A Descritpion of the data file

The file `source.dat` contains data needed to compute the source term f_i in eq. (3). These data come from a Near Field computation. The file has 212 lines, and each line contains three numbers t^p, f_1^p, f_2^p, $p = 1, \ldots 212$, where t^p is the time, and the source term $f_i(t^p)$ is related to f_i^p by: $f_i(t^p) = f_i^p/S$, where S is the surface of the repository.

The times t^p are in years, and the numbers f_i^p are in units of mole $/_{year}$.